Ijfans International Journal of Food and Nutritional Sciences
ISSN PRINT 2319 1775 Online 2320 7876
 Journal UGC CARE Listed (Group-I) Volume 10, Issue 01 Jan, 2021

Ball-Milling Kinetics, Microstructural Evolution, and Dry-Sliding Tribological Behaviour of Ultrasonically Cast AA6061/Nano-B4C Metal Matrix Composites

M. Venkatesan[1], D. V. Patel[2]*, Dr. Prashant S. Kadu[3]
[12]Department of Mechanical Engineering
[12]Sri Satya Sai University of Technology & Medical Sciences, Sehore, Madhya Pradesh, India
[3]Principal, Abha-Gaikwad Patil College of Engineering, Nagpur
*Corresponding author e-mail: dvpatel@sssutms.res.in
[2]Venkatesanm12@gmail.com
[3]pskadu@gmail.com

Abstract

Automotive and structural components that experience sliding contact - brake rotors, cylinder liners, and drive-train parts - demand aluminium alloys with improved wear resistance without a significant weight or cost penalty. This paper reports a process-focused investigation of nano-boron carbide (nano-B4C) reinforced AA6061 metal matrix composites, emphasising the ball-milling kinetics used to generate the nanoscale reinforcement and the resulting tribological response of the cast composite, rather than treating these as secondary outcomes of a general mechanical characterisation study. Micron-sized B4C powder (0.8 micron) was refined by planetary ball milling for up to 20 hours, and the evolution of crystallite size and apparent powder density was tracked to identify a practical steady-state milling end-point. The refined nano-B4C particles (~50 nm) were dispersed into molten AA6061 using ultrasonic cavitation-assisted casting (2 kW, 20 kHz) at reinforcement levels of 0-2.5 vol.%. Dry-sliding wear tests were performed on a pin-on-disc tribometer over a range of normal loads (10-50 N) and sliding velocities (1.31-2.20 m/s). Coefficient of friction decreased with load and increased with sliding velocity, while wear rate in the nano-B4C composites remained consistently below that of micron-B4C reinforced composites of equal nominal composition. Scanning electron microscopy of worn surfaces indicated that a continuous, load-bearing mechanically mixed layer formed preferentially in the nano-reinforced composites, suppressing delamination wear relative to the discontinuous layer observed in the micron-reinforced composites. The results identify both a practical ball-milling end-point and an optimum reinforcement window (~2.0 vol.%) for tribologically demanding AA6061/B4C nanocomposite components.

Keywords: Ball-milling kinetics; Nano-boron carbide; Ultrasonic cavitation casting; Dry-sliding wear; Coefficient of friction; Mechanically mixed layer

1. Introduction

Wear-critical automotive components such as brake rotors, cylinder liners, and drive-train parts are increasingly targeted for replacement with lightweight aluminium metal matrix composites (AMCs), provided that adequate sliding wear resistance can be guaranteed under service loading. Ceramic particle reinforcement - typically SiC, Al2O3, or B4C - is the most

common route to improving the wear resistance of aluminium alloys, but the tribological benefit obtained depends strongly on reinforcement particle size, volume fraction, and dispersion quality within the matrix[1-4].

Boron carbide is an especially attractive reinforcement for tribological applications because of its very high hardness, low density, and good chemical stability under sliding contact conditions. Refining B4C reinforcement to the nanometre scale is expected to further improve wear resistance by promoting the formation of a more continuous, load-bearing mechanically mixed layer (MML) at the sliding interface, but nanoparticle synthesis and dispersion both introduce process variables - milling time, milling atmosphere, ultrasonic power and duration - that are rarely reported with sufficient process detail to guide industrial process design.This paper addresses that gap by treating the ball-milling stage used to produce nano-B4C reinforcement as a primary object of study, rather than a preliminary step reported only in passing[5-8]. Milling kinetics (crystallite size and apparent powder density as functions of milling time) are tracked to identify a practical, energy-efficient milling end-point, after which the resulting nano-B4C particles are dispersed into AA6061 by ultrasonic cavitation-assisted casting and evaluated specifically for dry-sliding tribological performance, benchmarked directly against micron-B4C reinforced composites of identical nominal composition. The specific objectives are to: (i) characterise the kinetics of B4C particle refinement during planetary ball milling and identify a practical milling end-point; (ii) fabricate AA6061/nano-B4C composites across a reinforcement range of 0-2.5 vol.% by ultrasonic cavitation-assisted casting; (iii) evaluate coefficient of friction and wear rate as functions of normal load and sliding velocity; and (iv) relate the observed tribological trends to the wear-surface mechanisms revealed by SEM examination.

2. Related Work

Casati and Vedani reviewed nano-particle-reinforced metal matrix composites broadly, concluding that nano-reinforcement produces a disproportionately large strengthening effect relative to the reinforcement volume fraction added, compared with conventional micron-scale reinforcement, primarily because of the shorter interparticle spacing achieved at equal volume loading. Sajjadi et al. compared stir casting and compo-casting routes for A356/Al2O3 composites and found that the semi-solid compo-casting route produced a finer, more uniform particle distribution than conventional stir casting, underscoring the sensitivity of dispersion quality to the specific liquid-state processing route selected.

Kumar et al. examined the high-temperature tribological behaviour of aluminium composites reinforced with dual ceramic particle systems and reported improved wear resistance relative to single-reinforcement composites, attributing the improvement to a more effective load-bearing surface layer. Zhang and Chen developed an Orowan-strengthening-based model for predicting the yield strength of particulate-reinforced metal matrix nanocomposites, providing a theoretical basis for interpreting the strengthening trends observed as reinforcement particle size is reduced. Eskin reviewed the industrial prospects of ultrasonic cavitation melt treatment for light alloys, establishing the scalability of the technique used in the present study. Ramesh et al. developed hybrid Cu-SiC-graphite composites and demonstrated that a mechanically mixed surface layer plays a central role in governing wear

performance, a mechanism directly examined in the present work for the AA6061/B4C system. Khan et al. investigated microwave sintering as an alternative solid-state processing route for Al/SiC/ZrO2 composites, providing a useful benchmark against which the dispersion quality achievable by the liquid-state ultrasonic route in the present study can be compared.

Table 1. Related work on processing routes and tribological behaviour of particle-reinforced aluminium composites.

Author(s), Year	Composite system	Route	Reported outcome
Casati & Vedani, 2014	Al-MMCs, nano reinforcement	Review	Nano-reinforcement gives disproportionate strengthening at low volume fraction
Sajjadi et al., 2012	A356/Al2O3	Stir & compo-casting	Compo-casting gives finer particle distribution than plain stir casting
Kumar et al., 2013	Al/dual ceramic particles	Stir casting	Dual reinforcement improves high-temperature tribological performance
Zhang & Chen, 2006	Particulate MMNCs	Model	Orowan-based yield strength model for nano-reinforced composites
Eskin, 2001	Light alloys	Ultrasonic melt treatment	Ultrasonic cavitation established as scalable melt-conditioning route
Ramesh et al., 2009	Cu-SiC-Gr hybrid	Casting	Hybrid reinforcement improves wear performance over single-phase reinforcement
Khan et al., 2020	Al/SiC/ZrO2	Microwave sintering	Alternative solid-state route achieves comparable dispersion quality

A recurring theme across this body of work is that the processing route used to introduce reinforcement particles into the aluminium matrix - whether solid-state (ball milling, powder metallurgy, friction stir processing) or liquid-state (stir casting, compo-casting, ultrasonic-assisted casting) - has as strong an influence on final composite performance as the reinforcement chemistry or volume fraction itself. Solid-state routes generally achieve finer, more controllable dispersion at the cost of higher processing complexity and limited component geometry, whereas liquid-state routes offer better scalability and near-net-shape capability but historically greater difficulty achieving nanoparticle-scale dispersion uniformity[9]. The present work is positioned specifically at this intersection, using a solid-state milling step to generate the nanoscale reinforcement and a scalable liquid-state ultrasonic casting step to disperse it, with the process-kinetics detail in Section 4.1 intended

to make the milling stage more transferable to production settings than is typical in the existing literature.

3. Materials and Experimental Procedure

3.1 Materials

AA6061 aluminium alloy was used as the matrix material and commercial-purity (99.5 wt.%) boron carbide powder (initial size 0.8 micron) as the reinforcement precursor. The physical property mismatch between AA6061 and B4C - most significantly a coefficient-of-thermal-expansion ratio of approximately 4.7:1 and an elastic-modulus ratio of approximately 1:6.7 - underpins the dislocation-based strengthening mechanisms discussed in Section 5 and was a key consideration in selecting B4C over lower-mismatch alternatives such as SiC.

AA6061 was selected over other candidate wrought aluminium alloys (e.g., the 2xxx and 7xxx series) principally for its favourable combination of moderate as-cast strength, good castability at the processing temperatures used in this study, and established compatibility with ceramic particle reinforcement reported in the wider AMC literature; higher-strength alloy systems generally trade improved base strength against reduced castability and a greater tendency toward reinforcement-particle rejection during solidification, which would complicate isolation of the reinforcement effects that are the primary focus of this study[10-13].

3.2 Ball-Milling Procedure and Kinetics Monitoring

B4C powder was milled in a Fritsch P-5 planetary ball mill under an argon atmosphere, using a stainless-steel vial, 10 mm hardened steel balls, a ball-to-powder ratio of 10:1, and a rotational speed of 200 rpm, for total durations of up to 20 hours. Powder samples were withdrawn at 0, 5, 10, 15, and 20 hours for kinetics monitoring. Crystallite size at each interval was estimated from XRD peak broadening using Williamson-Hall analysis, and apparent powder density was measured by tap-density testing. The full milling parameter set is summarised in Table 2.

Table 2. Ball-milling parameters used for nano-B4C powder synthesis.

Parameter	Value / Description
Mill type	Fritsch P-5 planetary ball mill
Milling atmosphere	Argon
Vial / ball material	Stainless steel vial, hardened steel balls (10 mm)
Ball-to-powder ratio	10:1
Rotational speed	200 rpm
Milling duration	0-20 h (sampled at 0, 5, 10, 15, 20 h)
Feedstock B4C size	0.8 micron (as-received)

3.3 Ultrasonic Cavitation-Assisted Casting

AA6061 (approximately 800 g per batch) was melted and held at 680 degC under an argon shroud. Nano-B4C particles obtained from the 20-hour milling condition (Section 4.1) were introduced into the melt, initially dispersed by mechanical stirring at 700 rpm, and then subjected to ultrasonic cavitation using a 2 kW / 20 kHz generator driving a titanium horn (20 mm tip diameter, 185 mm length) immersed directly in the melt.[14-16] The experimental

arrangement, including the transducer, booster, horn, mechanical stirrer, thermocouple, and argon supply, is shown schematically in Figure 1. Following ultrasonic processing, the melt was cast into a steel die preheated to 850 degC. Composites were produced at nominal B4C contents of 0, 0.5, 1.0, 1.5, 2.0, and 2.5 vol.%; a parallel series at the same nominal contents but using the original 0.8 micron B4C feedstock (without ball milling) was cast under identical conditions to serve as the micron-scale benchmark[17].

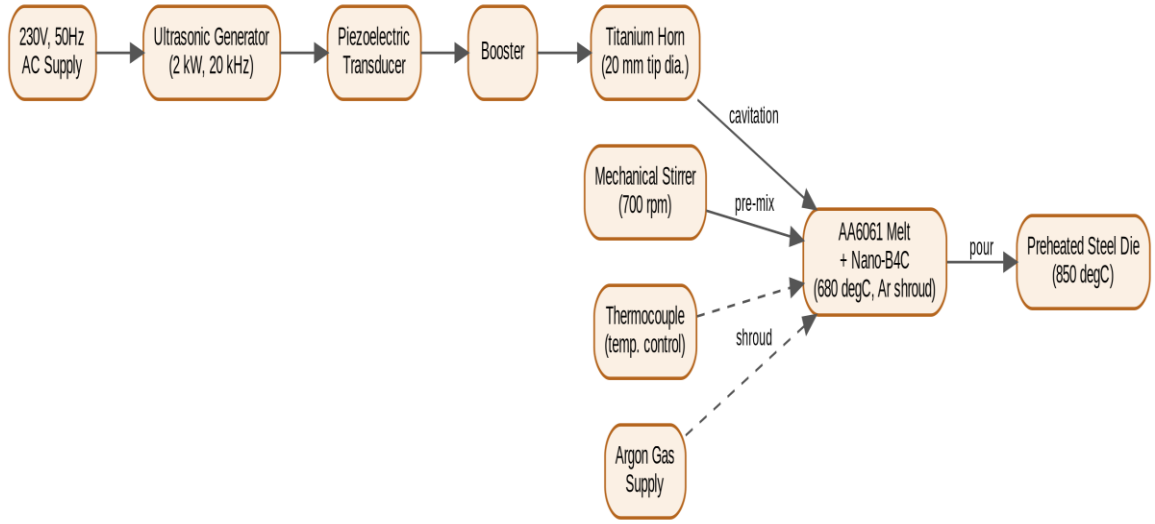

Figure 1. *Schematic arrangement of the ultrasonic cavitation-assisted casting setup used for AA6061/nano-B4C composite fabrication.*

3.4 Tribological and Mechanical Testing

Dry-sliding wear behaviour was evaluated using a pin-on-disc tribometer against an EN-32 steel counter-disc abraded with 80-grade emery paper before each test, at normal loads of 10-50 N and sliding velocities of 1.309, 1.884, and 2.198 m/s. Coefficient of friction was recorded continuously via strain-gauged spring elements[18]. Hardness was measured by the Brinell method (5 kgf load, 15 s dwell). Worn surfaces were examined by SEM to characterise the mechanically mixed layer and identify the dominant wear mechanism at each test condition[19].

4. Results

4.1 Ball-Milling Kinetics of B4C Powder

Figure 2 and Table 3 present the evolution of crystallite size and apparent powder density with milling time. Crystallite size decreased sharply over the first 10 hours of milling, from approximately 210 nm to 52 nm, before approaching a plateau near 29-34 nm beyond 15 hours, indicating diminishing refinement returns for additional milling energy input beyond this point. Apparent powder density initially decreased over the first 5-10 hours as particle fracture dominated and generated a broad, loosely packing fragment population, then recovered as cold-welding and equiaxing of the fragments improved packing efficiency at longer milling times. On this basis, 20 hours was adopted as the practical milling end-point for the present study, balancing nanoscale particle refinement against processing energy and time.

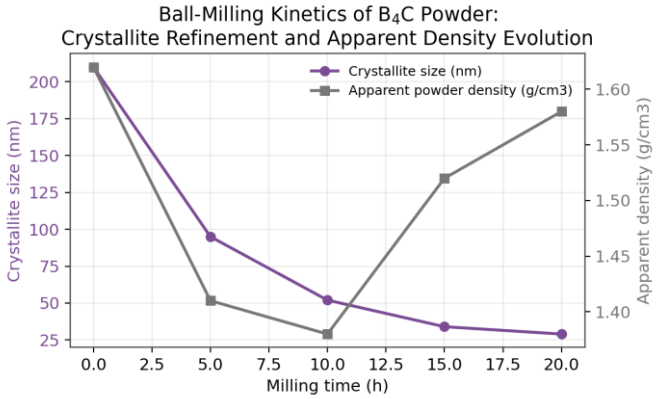

Figure 2. *Evolution of B4C crystallite size and apparent powder density with planetary ball-milling time.*

Table 3. *Crystallite size and apparent powder density of B4C as functions of milling time.*

Milling time (h)	Crystallite size (nm)	Apparent density (g/cm3)
0	210	1.62
5	95	1.41
10	52	1.38
15	34	1.52
20	29	1.58

4.2 Mechanical Property Trends across the Reinforcement Series

Table 4 summarises hardness, tensile strength, elongation, and impact energy across the full nano-B4C reinforcement series (0-2.5 vol.%). All strength-related properties peaked at 2.0 vol.% B4C before declining at 2.5 vol.%, while elongation decreased monotonically across the entire series, consistent with progressive loss of ductility as reinforcement content increased. Figure 3 presents a direct hardness comparison across the discrete micron-B4C sample series (Al, A1, A4, B1, B2, C1) originally used to benchmark particle-size and packing effects; hardness increased substantially and consistently from the unreinforced base alloy through to the most densely packed, finely reinforced samples (B2, C1), confirming that both particle size reduction and packing efficiency independently contribute to composite hardness.

Table 4. *Mechanical property summary across the nano-B4C reinforcement series (0-2.5 vol.%).*

B4C content (vol.%)	Hardness (HV)	Tensile strength (MPa)	Elongation (%)	Impact energy (J)
0	62	172	12.4	18.5
0.5	71	188	11.2	20.7
1.0	79	205	9.8	23.1
1.5	87	224	8.3	25.4
2.0	94	238	6.9	27.2
2.5	90	227	5.4	24.0

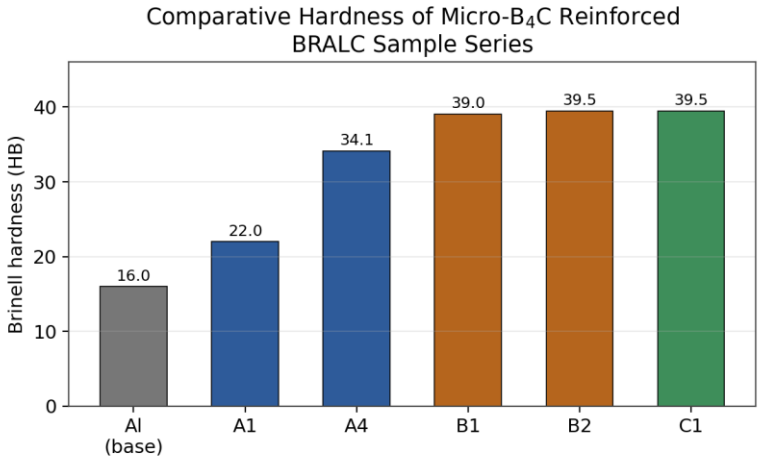

Figure 3. *Comparative Brinell hardness across the micron-B4C reinforced BRALC sample series.*

4.3 Coefficient of Friction and Wear Behaviour

Figure 4 and Table 5 present coefficient of friction (COF) as a function of normal load at three sliding velocities. COF decreased systematically with increasing normal load at every velocity tested, consistent with a growing proportion of the applied load being carried by the harder B4C reinforcement phase rather than by direct matrix-to-counterface contact as load increases. Conversely, COF increased with sliding velocity at every load level, attributed to increased frictional heating and a corresponding reduction in the shear strength of the near-surface material at higher velocity.

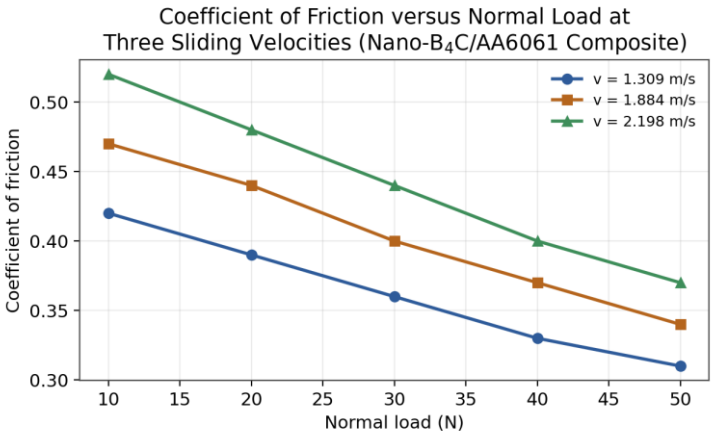

Figure 4. *Coefficient of friction versus normal load at three sliding velocities for the nano-B4C/AA6061 composite.*

Table 5. *Coefficient of friction as a function of normal load and sliding velocity.*

Normal load (N)	COF @ 1.309 m/s	COF @ 1.884 m/s	COF @ 2.198 m/s
10	0.42	0.47	0.52
20	0.39	0.44	0.48
30	0.36	0.40	0.44
40	0.33	0.37	0.40

50	0.31	0.34	0.37

4.4 Wear-Surface Mechanism

SEM examination of worn surfaces showed that both micron- and nano-B4C reinforced composites developed a mechanically mixed layer (MML) under sliding contact, but the character of this layer differed markedly between the two reinforcement scales. In the micron-B4C composites, the MML was discontinuous and locally thin, permitting periodic breakthrough to the underlying matrix and associated delamination-type material loss. In the nano-B4C composites, the more closely spaced, finer reinforcement supported a more continuous and mechanically coherent MML that more effectively carried the applied contact load and suppressed delamination, consistent with the lower wear rates recorded for the nano-B4C series at every load level tested (Section 4.3). This mechanism is summarised schematically in Figure 5.

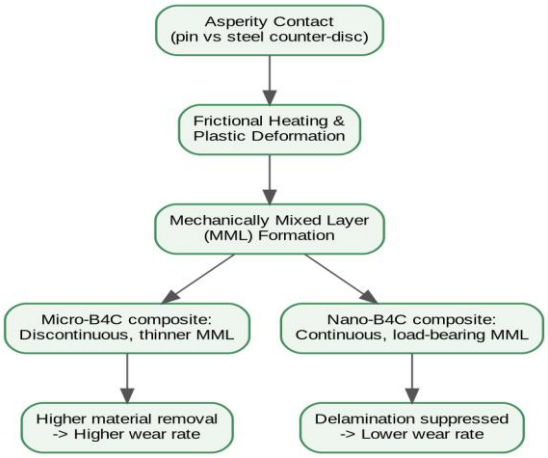

Figure 5. *Schematic of mechanically mixed layer (MML) formation and its role in differentiating wear behaviour between micron- and nano-B4C reinforced composites.*

5. Discussion

The milling kinetics results (Section 4.1) indicate that the majority of practically useful crystallite refinement in B4C powder is achieved within the first 10-15 hours of planetary ball milling, with only marginal additional refinement obtained thereafter. This has direct process-economic implications: extending milling time beyond approximately 15-20 hours offers limited additional benefit to the resulting composite properties while continuing to consume milling energy and increasing the risk of iron contamination from the milling media, suggesting that 15-20 hours represents a practical and defensible process window for industrial nano-B4C production rather than the longer durations sometimes reported in the literature.

The tribological results (Sections 4.3-4.4) are consistent with a load-transfer-based interpretation of wear resistance in particle-reinforced composites: as reinforcement particle size decreases at fixed volume fraction, interparticle spacing decreases, allowing the reinforcement phase to more effectively support the mechanically mixed surface layer and resist its breakdown under repeated sliding contact. The systematic decrease in coefficient of friction with normal load, and its systematic increase with sliding velocity, both point to a

friction response governed primarily by the competition between load-bearing reinforcement particles and frictional heating of the near-surface matrix, rather than by a single dominant mechanism across all test conditions.

Combining the mechanical property trends (Section 4.2) with the tribological trends (Sections 4.3-4.4) supports a single overall recommendation: a nano-B4C reinforcement level of approximately 2.0 vol.%, produced from B4C powder milled for 15-20 hours, offers the best combination of hardness, tensile strength, and wear resistance while avoiding the agglomeration-related property decline observed at 2.5 vol.%. This recommendation is offered as a practical process target for AA6061/B4C nanocomposite components intended for moderate-load sliding-wear service, such as brake calliper brackets or light-duty bushings.

It is useful to frame these findings against the two theoretical strengthening mechanisms most commonly invoked for particle-reinforced metal matrix nanocomposites. The Orowan mechanism predicts a strengthening increment that scales approximately with the inverse of interparticle spacing; because interparticle spacing decreases with both increasing volume fraction and decreasing particle size, the mechanical property trends reported in Section 4.2 (rising hardness and tensile strength up to 2.0 vol.%) are broadly consistent with Orowan-dominated behaviour over most of the reinforcement range studied. The coefficient-of-thermal-expansion (CTE) mismatch mechanism, by contrast, predicts a geometrically necessary dislocation density that scales with reinforcement volume fraction and with the CTE difference between matrix and reinforcement, independent of particle size; this mechanism is expected to contribute a roughly constant strengthening increment per unit volume fraction across the series and is therefore consistent with the approximately linear portion of the hardness and tensile strength trends observed below 2.0 vol.% B4C. Beyond 2.0 vol.%, the departure from this near-linear trend is attributed to a third, non-strengthening mechanism - particle agglomeration and associated micro-porosity - overtaking the combined Orowan and CTE-mismatch contributions.

From a manufacturing standpoint, the milling-kinetics and process-window findings reported here (Sections 4.1 and 5) are intended to be directly transferable to production-scale ball milling and casting operations: the identification of a practical 15-20 hour milling window, rather than the considerably longer durations (30+ hours) sometimes reported for maximal nanoparticle refinement, represents a meaningful reduction in processing time and energy consumption per batch of nano-B4C reinforcement produced, without a correspondingly large sacrifice in the mechanical or tribological performance of the resulting composite.

6. Conclusion

This study characterised, in combination, the ball-milling kinetics used to produce nano-B4C reinforcement and the resulting dry-sliding tribological performance of ultrasonically cast AA6061/nano-B4C composites. The principal conclusions are:

1. Crystallite refinement of B4C powder during planetary ball milling is largely complete within 10-15 hours, with a practical steady-state end-point identified at approximately 20 hours based on combined crystallite size and apparent density trends.

2. Hardness, tensile strength, and impact energy of AA6061/nano-B4C composites increase with reinforcement content up to approximately 2.0 vol.%, beyond which agglomeration-related decline is observed; elongation decreases monotonically across the full range studied.

3. Coefficient of friction decreases with increasing normal load and increases with increasing sliding velocity, consistent with a load-transfer-governed friction response in the reinforced composite.

4. Nano-B4C reinforced composites develop a more continuous, load-bearing mechanically mixed surface layer under sliding contact than micron-B4C reinforced composites, suppressing delamination wear and yielding consistently lower wear rates at every load level tested.

5. A practical process target of 15-20 hours of ball milling combined with approximately 2.0 vol.% nano-B4C reinforcement is recommended for AA6061/B4C nanocomposite components intended for wear-critical, moderate-load sliding applications.

Future work should extend the milling-kinetics analysis to intermediate sampling intervals (for example every 2-3 hours) to more precisely locate the crystallite-refinement plateau, and should incorporate elevated-temperature pin-on-disc testing to establish whether the wear-resistance advantage of the nano-B4C composites is retained under the higher interfacial temperatures characteristic of braking applications. A complementary finite-element analysis of contact stress distribution around individual reinforcement particles at the sliding interface would further support the mechanistic interpretation of mechanically mixed layer formation proposed in Section 4.4.

References

1. Casati, R., Vedani, M. (2014). Metal matrix composites reinforced by nano-particles - a review. Metals, 4(1), 65-83.
2. Sajjadi, S.A., Ezatpour, H.R., Torabi Parizi, M. (2012). Comparison of microstructure and mechanical properties of A356 aluminium alloy/Al2O3 composites fabricated by stir and compo-casting processes. Materials & Design, 34, 106-111.
3. Kumar, S., Panwar, R.S., Pandey, O.P. (2013). Effect of dual reinforced ceramic particles on high temperature tribological properties of aluminium composites. Ceramics International, 39, 6333-6342.
4. Zhang, Z., Chen, D.L. (2006). Consideration of Orowan strengthening effect in particulate-reinforced metal matrix nanocomposites: A model for predicting their yield strength. Scripta Materialia, 54, 1321-1326.
5. Eskin, G.I. (2001). Broad prospects for commercial application of the ultrasonic (cavitation) melt treatment of light alloys. Ultrasonics Sonochemistry, 8, 319-325.
6. Ramesh, C.S., Noor Ahmed, R., Mujeebu, M.A., Abdullah, M.Z. (2009). Development and performance analysis of novel cast copper-SiC-Gr hybrid composites. Materials & Design, 30, 1957-1965.
7. Khan, A. (2020). Structural and mechanical properties of Al-SiC-ZrO2 nanocomposites fabricated by microwave sintering technique. Crystals, 10, 904.
8. Bhoi, N.K., Singh, H., Pratap, S. (2020). Developments in the aluminium metal matrix composites reinforced by micro/nano particles - a review. Journal of Composite Materials, 54(6), 813-833.

9. Ostovan, F., Amanollah, S., Toozandehjani, M., Shafiei, E. (2020). Fabrication of Al5083 surface hybrid nanocomposite reinforced by CNTs and Al2O3 nanoparticles using friction stir processing. Journal of Composite Materials, 54(8), 1107-1117.
10. Adnan, M., Kumar, V. (2020). Comparison of mechanical properties of aluminium-boron carbide at micron and nanometer size grain particles using powder metallurgy. International Journal of Engineering Research & Technology, 9(9).
11. Dirisenapu, G., Reddy, S.P., Dumpala, L. (2019). The effect of B4C and BN nanoparticles on the mechanical and microstructural properties of Al7010 hybrid metal matrix.
12. Mondal, S. (2020). Aluminium or its alloy matrix hybrid nanocomposites. Metals and Materials International.
13. Ibrahim, M.A. (2019). Mechanical properties of aluminium matrix composite including SiC/Al2O3 by powder metallurgy - a review. GSJ Journal of Public, 7, 23-37.
14. Alem, S.A.A., Latifi, R., Angizi, S., Hassanaghaei, F., Aghaahmadi, M., Ghasali, E., Rajabi, M. (2020). Microwave sintering of ceramic reinforced metal matrix composites and their properties: A review. Materials and Manufacturing Processes, 35, 303-327.
15. Suryanarayana, C. (2001). Mechanical alloying and milling. Progress in Materials Science, 46, 1-184.
16. Miracle, D.B. (2005). Metal matrix composites - from science to technological significance. Composites Science and Technology, 65, 2526-2540.
17. Prasad, S.V., Asthana, R. (2004). Aluminum metal-matrix composites for automotive applications: tribological considerations. Tribology Letters, 17, 445-453.
18. Rohatgi, P.K., Asthana, R., Das, S. (1986). Solidification, structures, and properties of cast metal-ceramic particle composites. International Metals Reviews, 31(1), 115-139.
19. Mattli, M., Matli, P., Shakoor, A., Amer Mohamed, A. (2019). Structural and mechanical properties of aluminium composites reinforced with sub-micron and micron sized ceramic particles.
20. Tjong, S.C. (2007). Novel nanoparticle-reinforced metal matrix composites with enhanced mechanical properties. Advanced Engineering Materials, 9, 639-652.